

## Study of Oxidation-State Contrast in Gallium Dichloride by Synchrotron X-ray Anomalous Scattering

BY A. P. WILKINSON AND A. K. CHEETHAM

*Chemical Crystallography Laboratory, University of Oxford, 9 Parks Road, Oxford OX1 3PD, England*

AND D. E. COX

*Physics Department, Brookhaven National Laboratory, Upton, Long Island, New York 11973, USA*

(Received 25 April 1990; accepted 17 September 1990)

### Abstract

Synchrotron X-ray powder diffraction data have been collected on mixed-valence gallium dichloride,  $\text{Ga}^{\text{I}}\text{Ga}^{\text{III}}\text{Cl}_4$ , at several wavelengths between 1.2481 and 1.1957 Å, the latter being very close to the Ga *K* edge. A significant difference in the  $f'(E)$  curves is observed between the  $\text{Ga}^{\text{I}}$  and  $\text{Ga}^{\text{III}}$  sites, within 10 eV of the edge. This result is consistent with an oxidation-state shift of up to 8 eV, with the  $\text{Ga}^{\text{I}}$  edge at a lower energy, but may also reflect a difference in the forms of the  $f'(E)$  curves for  $\text{Ga}^{\text{I}}$  and  $\text{Ga}^{\text{III}}$  in the vicinity of the edge.

### Introduction

The availability of tunable synchrotron X-ray sources has opened up many new possibilities for diffraction studies, particularly in relation to the use of anomalous scattering. A number of experiments have been carried out to determine the wavelength and scattering-angle dependence of the anomalous-scattering corrections,  $f'(E)$  and  $f''(E)$ , especially with single crystals, and the use of powder diffraction for such experiments has been demonstrated for  $\text{Yb}_2\text{O}_3$  (Will, Masciocchi, Hart & Parrish, 1987). In addition, there has also been some work on the anisotropic nature of such corrections (Templeton & Templeton, 1982, 1985). The solution of protein structures is probably the most common application of anomalous scattering in crystallography, but a few applications outside this area have also been reported. Some involve the use of single crystals, for example the refinement of cation occupancies in situations where several species occupy the same crystallographic site, as in the 2212 Bi–Sr–Ca–Cu superconductors (Lee, Gao, Sheu, Petricek, Restori, Coppens, Darovskikh, Phillips, Sleight & Subramanian, 1989). However, there is a growing emphasis on the use of powder methods, which offer an attractive alternative in cases where suitable crystals are not available, and are less prone to beam

instabilities and instrumental alignment problems. Recent examples include the study of elemental distributions in  $\text{Fe}_{0.5}\text{Co}_{0.48}\text{V}_{0.2}$  (Williams, Kwei, Ortiz, Karnowski & Warburton, 1990),  $\text{La}_{0.9}\text{Gd}_{0.9}\text{Sr}_{0.2}\text{CuO}_4$  (Kwei, Von Dreele, Williams, Goldstone, Lawson & Warburton, 1990) and doped  $\text{YBa}_2\text{Cu}_3\text{O}_7$  (Howland, Geballe, Laderman, Fischer-Colbrie, Scott, Tarascon & Barboux, 1989), the refinement of independent temperature factors for species on the same cation site in yttrium-doped  $\text{ZrO}_2$  (Moroney, Thompson & Cox, 1988), and distinguishing between elements of similar atomic number in  $\text{EuSm}_2\text{O}_4$  (Attfield, 1990). Such information can sometimes be obtained by the combined analysis of neutron and conventional X-ray data, but the role of neutron diffraction is limited in some cases by absorption or lack of contrast. Multi-wavelength X-ray experiments are free of such limitations and offer the possibility of element-selective diffraction for all but a few elements of low atomic number.

A recent and exciting development in the use of anomalous scattering with powders is the examination of the ordering of atoms in different oxidation states. This relies upon the rapid variation in  $f'$  and  $f''$  as a function of X-ray energy near an absorption edge, combined with a shift in the edge for different oxidation states. This shift is typically a few eV, sufficient to produce a measurable difference in anomalous-scattering factors for the different oxidation states if the experiment is performed at an energy near to an edge. Experiments of this type have been carried out at the  $L_{\text{III}}$  edge of Eu in  $\text{Eu}_3\text{O}_4$  (Attfield, 1990) and at the *K* edge of Cu in  $\text{YBa}_2\text{Cu}_3\text{O}_{6+x}$  (Kwei, Von Dreele, Williams, Goldstone, Lawson & Warburton, 1990). However, care is required in the interpretation and quantification of such measurements in terms of a simple valence model, and we have therefore chosen to carry out a detailed study of the well characterized mixed-valence compound,  $\text{Ga}^{\text{I}}\text{Ga}^{\text{III}}\text{Cl}_4$  (Garton & Powell, 1957; Schmidbaur, Nowak, Bublak, Burkert, Huber & Müller, 1987), in which the  $\text{Ga}^{\text{I}}$  enjoys eightfold

dodecahedral coordination and Ga<sup>III</sup> is tetrahedrally coordinated. Our results illustrate some of the difficulties that are involved in experiments of this type.

### Experimental

GaCl<sub>2</sub> was prepared by the reaction of Ga metal and dry HgCl<sub>2</sub> in a sealed Pyrex vessel at 453 K. The Hg produced was decanted into a side arm and removed. The resulting GaCl<sub>2</sub> was ground under an inert atmosphere and the white powder was packed into a 0.3 mm diameter glass capillary, which was immediately sealed. This procedure is necessary to prevent the decomposition due to hydrolysis; in addition, the use of a capillary, rather than a flat-plate sample, minimizes preferred orientation effects.

The data collection was carried out using the powder diffractometer on beam line X7A at the National Synchrotron Light Source, Brookhaven National Laboratory. An Si(111) channel-cut monochromator was used to provide tunable monochromatic radiation with an estimated bandpass of 2 eV. Several different instrumental configurations were explored for data collection, including the use of a 0.04° receiving slit in front of a solid-state detector, a Ge(220) analyser crystal and a solid-state detector, and Ge(220) or LiF(200) analyser crystals placed in front of a scintillation counter. In all cases the sample was oscillated by 10–20° during data collection. Initially, the solid-state detector was not available and a Ge(220) analyser and scintillation counter were used. This gave excellent resolution and peak-to-background discrimination, but it was found that this configuration produced data showing signs of poor powder averaging. The very small acceptance angle of the analyser crystal (0.003°), combined with a rather large particle size, lead in some instances to a poor sampling of crystallite orientations, even with sample oscillation. When the Ge(220) analyser crystal was replaced by an LiF crystal for the collection of a series of low-angle peaks showing high sensitivity to  $f'$ , data of better reproducibility were obtained, albeit with significantly lower resolution, the larger acceptance angle of the LiF(200) reflection (0.02°) helping to give improved powder averaging. The subsequent availability of a Peltier-cooled solid-state detector (resolution 300 eV FWHM) allowed the collection of high-quality data using a single slit with an acceptance angle of 0.04°. Here the large acceptance angle of the slit eliminated problems with powder averaging. The solid-state detector and slit arrangement gave the best combination of count rate, resolution and peak-to-background ratio, the superior energy resolution of the detector being especially valuable in discriminating against Ga  $K\alpha$  fluorescent radiation close to the Ga edge. Details of the data sets, which comprise several extended scans

Table 1. *Details of data collection at different wavelengths*

$\lambda$ (Å)	Energy (eV)	Angular range (°)	Detector*	Step size (°)
1.2481 (1)	9933.9	10.20–10.80	LiF + SC	0.01
		19.00–20.20		
		20.80–21.40		
1.24783 (5)	9936.1	10.00–55.38	Slits + SS	0.01
1.24768 (5)	9937.3	10.00–50.49	Ge + SC	0.005
1.2224 (1)	10142.8	10.00–10.60	LiF + SC	0.01
		18.80–19.80		
		20.40–21.00		
1.2023 (1)	10312.4	9.80–10.40	LiF + SC	0.01
		18.30–19.50		
		20.00–20.60		
1.19761 (7)	10352.8	9.70–10.32	Slits + SS	0.01
		11.60–12.16		
		13.54–14.64		
		18.23–19.30		
		20.04–20.60		
		21.42–23.15		
1.19756 (5)	10353.2	9.00–14.00	Ge + SS	0.005
		18.06–41.885		
1.1974 (1)	10354.6	9.80–10.40	LiF + SC	0.01
		18.20–19.40		
		19.90–20.50		
1.1968 (1)	10359.8	9.80–10.40	LiF + SC	0.01
		18.20–19.22		
		19.90–20.50		
1.19639 (5)	10363.3	9.50–50.56	Slits + SS	0.01
1.19614 (7)	10365.5	10.00–50.89	Ge + SC	0.01
1.19568 (5)	10369.5	9.00–51.72	Slits + SS	0.01

\*Ge/LiF – a Ge(220)/LiF(200) crystal scattering into the detector; SS – solid-state detector; SC – scintillation counter; Slits – a receiving slit used instead of an analyser crystal.

and a number of shorter ones over selected peaks, are given in Table 1.

For data collection close to an absorption edge, it is clearly important that fluctuations in energy due to factors such as the movement of the source and crystal heating effects should be as small as possible. Past experience, based on repeated calibration with an Si standard over a period of several days while working in the vicinity of the Ga  $K$  edge (10370 eV), indicates that the long-term fluctuations in energy are less than 2 eV under the experimental conditions used. Such a change would have no measurable effect on the intensities, except that due to small changes in anomalous scattering, although there could be small shifts in the peak positions of less than 0.01° over the course of an extended scan. However, no indication of any such shifts was noticed in our data analysis.

Before commencing the data collection, the absorption-edge position was determined approximately by carrying out a monochromator scan through the edge with an ionization chamber placed behind the sample. The on-edge data collections were performed at slightly higher energies than the bottom of the observed absorption feature. For the full data sets, the wavelength calibration was carried out using an Si standard, but the wavelengths for the partial data sets were determined from the measured lattice constants of GaCl<sub>2</sub>. The precision of the calibration procedure was about 0.5 eV for a measurement involving the Ge(220) analyser crystal, and slightly

lower for the other arrangements. Data collection proved to be impracticable at energies slightly higher than 10370 eV due to greatly enhanced absorption by the sample.

Rietveld analysis of the data was carried out using the Generalized Structure Analysis System, *GSAS* (Larson & Von Dreele, 1987). Neutral-atom scattering factors were used for all atoms after initial refinements using  $f(\text{Ga})$  and  $f(\text{Ga}^{3+})$  for the  $\text{Ga}^{\text{I}}$  and  $\text{Ga}^{\text{III}}$  sites, respectively, showed a difference in  $f'$  for the two cation sites, even for data sets collected well away from the absorption edge. *GSAS* offers the possibility of simultaneously refining a model against all the available data sets. In practice, we chose to refine a single structural model against all of the data sets that contained sufficient Bragg peaks to allow independent refinement of separate  $f'$  for the two cation sites. In addition, a number of partial data sets collected with the LiF analyser crystal were used in the refinement of a model with  $f'$  constrained to be the same for both cation sites, using the structural model derived from the complete data sets. The structural starting model was obtained from Schmidbaur, Nowak, Bublak, Burkert, Huber & Müller (1987). In all of the refinements,  $f''$  was fixed at the value reported for GaAs (Fukamachi, Hosoya, Kawamura & Okunuki, 1977) corresponding as closely as possible to the refined  $f'$ . This was done because free refinement of  $f''$  was either unstable or gave physically unreasonable parameters, due to the low sensitivity of the powder diffraction method to  $f''$ .

For the extended off-edge data sets at 9936.1 and 9937.3 eV, an initial refinement of all atomic coordinates,  $f'(\text{Ga}^{\text{I}})$  and  $f'(\text{Ga}^{\text{III}})$ , and the isotropic thermal parameters,  $U_{\text{iso}}$ , showed that the thermal parameters correlated strongly with  $f'$ . With  $f'$  fixed at the Cromer & Liberman (1970, 1981) values, an independent refinement of  $U_{\text{iso}}$ 's gave an almost identical goodness-of-fit and a poorly defined set of temperature factors. The problem of excessive correlation between  $f'$  and  $U_{\text{iso}}$ 's has been noted elsewhere and has been handled by fixing  $U_{\text{iso}}$  using information other than the X-ray data. Kwei, Von Dreele, Williams, Goldstone, Lawson & Warburton (1990) used temperature factors obtained from time-of-flight neutron diffraction data, which typically cover a large range in  $\sin(\theta/\lambda)$  and allow the determination of precise  $U_{\text{iso}}$ 's. Attfield (1990) fixed the temperature factors at a reasonable value in his refinement of  $\text{Eu}_3\text{O}_4$ ; this is to be avoided if possible due to the sensitivity of the derived  $f'$  values to the choice of temperature factors. In order to circumvent this problem in the present work, the temperature factors from the single-crystal structure determination of Schmidbaur, Nowak, Bublak, Burkert, Huber & Müller (1987) were used in our refinements, even

though their data were collected at the slightly lower temperature of 238 K. This appears to be a reasonable approach since the refined values of  $f'$  for the different cation sites are in close agreement for the off-edge data sets, as one would expect for a correct choice of relative temperature factors. No absorption correction was applied to any of the data as it was found that, over the  $\sin(\theta/\lambda)$  range used, the absorption correction varies only slightly with angle and correlates highly with the scale factor; it was therefore sufficient to refine only the latter.

### Results and discussion

The atomic coordinates obtained from the full data sets are compared with the single-crystal results of Schmidbaur, Nowak, Bublak, Burkert, Huber & Müller (1987) in Table 2, and selected bond lengths and angles are compared in Table 3. Some profile fits and difference plots are shown in Fig. 1. Our atomic coordinates are not in particularly good agreement with the single-crystal findings. In part this may stem from the different temperatures that were used for the experiments, but an analysis of the coordinates derived from independent refinements with the separate powder data sets suggests that the e.s.d.'s may be underestimated by a factor of 3–5. This is also consistent with the results of half-normal probability plots (Abrahams & Keve, 1971). However, an inspection of the bond lengths confirms that the structures are nevertheless in reasonable accord.

The final values of  $f'$  from all the refinements are given in Table 4. The most striking feature of the results is that, while the difference between the refined values of  $f'$  for  $\text{Ga}^{\text{I}}$  and  $\text{Ga}^{\text{III}}$  is negligible for the extended off-edge data sets, it is large (up to  $\sim 3$  e) and significant, even allowing for an underestimation of the e.s.d.'s, for data sets collected within approximately 10 eV of the edge (Fig. 2). This can be broadly interpreted as stemming from an absorption edge shift between the two cation sites, with the  $\text{Ga}^{\text{I}}$  edge at lower energy, as expected. The values from the partial data set refinements can be considered to represent the general behaviour of  $f'(E)$  for gallium, since there is little difference in  $f'$  for the two gallium sites away from the edge.

In order to extract the maximum amount of information from a study of this type, a knowledge of the behaviour of  $f'$  and  $f''$  in the region of the absorption edge is required. If reliable values are available, then it should be possible to estimate the relative X-ray absorption-edge positions. Theoretical values for the energy dependence of anomalous-scattering factors have been calculated by Cromer & Liberman (1970, 1981), and experimental values are available for a limited range of elements.

Table 2. Comparison between atomic coordinates of GaCl<sub>2</sub> from the present work and those of Schmidbauer *et al.* (1987)

The structural model from the joint refinement, with temperature factors constrained to those of the single-crystal study (below)

$$Pnma; a = 7.2235 (5), b = 9.7211 (6), c = 9.5421 (6) \text{ \AA}$$

	x	y	z
Ga <sup>III</sup>	0.25	0.0	0.1825 (2)
Ga <sup>I</sup>	0.6759 (2)	0.25	0.25
Cl(1)	0.3271 (3)	0.1762 (2)	0.0576 (2)
Cl(2)	0.0093 (2)	0.0419 (2)	0.3142 (2)

Individual profile *R* factors from the overall powder refinement

$\lambda$ (Å)	1.24783	1.24768	1.19761	1.19756	1.19639	1.19614	1.19568
<i>E</i> (eV)	9936.1	9937.3	10352.8	10353.2	10363.3	10365.5	10369.5
<i>R</i> <sub>wp</sub> (%)	10.5	23.7	10.1	15.5	8.0	24.5	5.7
<i>R</i> <sub>p</sub> (%)	8.5	18.2	7.8	12.2	6.5	19.7	4.6
<i>R</i> <sub>f</sub> (%)	7.5	14.2	4.1	9.9	10.9	16.8	17.6
Overall $\chi^2 = 1.99$							

The structural model from the single crystal data of Schmidbauer *et al.* (1987)

$$Pnma; a = 7.200 (1), b = 9.625 (1), c = 9.498 (1) \text{ \AA}$$

	x	y	z	<i>U</i> <sub>iso</sub> (Å <sup>2</sup> )
Ga <sup>III</sup>	0.25	0.0	0.1831 (1)	0.016
Ga <sup>I</sup>	0.6771 (1)	0.25	0.25	0.030
Cl(1)	0.3313 (2)	0.1767 (2)	0.0541 (1)	0.025
Cl(2)	0.0092 (2)	0.0438 (1)	0.3155 (2)	0.024

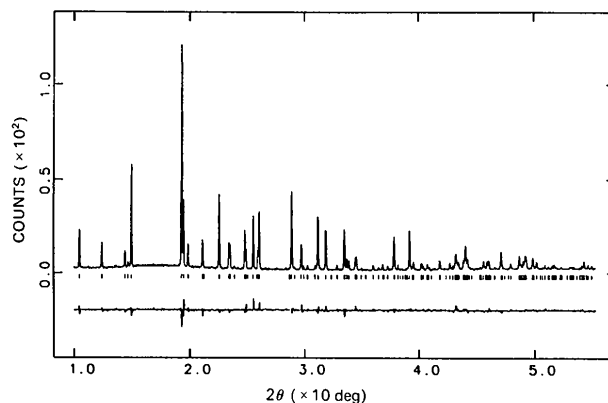
Table 3. Selected distances (Å) and bond angles (°) obtained from the powder experiment compared with those of the single-crystal study by Schmidbauer *et al.* (1987)

	Powder results	Single crystal
Ga <sup>III</sup> —Cl(1)	2.159 (2)	2.177 (1)
Ga <sup>III</sup> —Cl(2)	2.184 (2)	2.182 (2)
Ga <sup>I</sup> —Cl(1)	3.199 (2)	3.187 (2)
Ga <sup>I</sup> —Cl(1)'	3.213 (2)	3.174 (2)
Ga <sup>I</sup> —Cl(2)'	3.197 (2)	3.170 (2)
Ga <sup>I</sup> —Cl(2)	3.204 (2)	3.191 (2)
Cl(1)—Ga <sup>III</sup> —Cl(2)	112.0 (1)	112.8 (1)
Cl(1)—Ga <sup>III</sup> —Cl(1)'	113.0 (1)	111.4 (1)
Cl(2)—Ga <sup>III</sup> —Cl(2)'	109.7 (1)	109.7 (1)
Cl(1)—Ga <sup>III</sup> —Cl(2)'	105.1 (1)	105.2 (1)

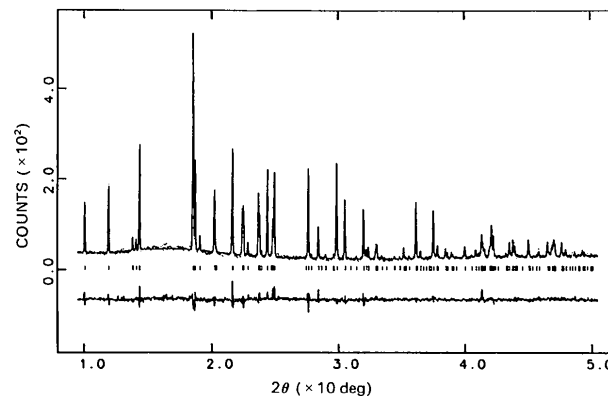
In the case of gallium, experiments have been carried out to determine  $f'(E)$  at the Ga *K* edge of GaAs and GaP (Fukamachi & Hosoya, 1975; Fukamachi, Hosoya, Kawamura & Okunuki, 1977), but the interpretation of our results on the basis of their values of  $f'$  has to be approached with some caution. The magnitudes of our observed values of  $f'$  for Ga<sup>I</sup>, close to the edge, are significantly different from those reported for Ga in GaAs, where the minimum value of  $f'$  is  $-10.6 e$ , determined with an experimental resolution of 1 eV (Fukamachi, Hosoya, Kawamura & Okunuki, 1977), as shown in Fig. 2. This could be due to differences in the near-edge structure. If the  $f'(E)$  curves for Ga<sup>I</sup> and Ga<sup>III</sup> in GaCl<sub>2</sub> are assumed to be the same shape, the observed differences in  $f'$  between the Ga<sup>I</sup> and Ga<sup>III</sup> sites would require an absorption-edge shift of about 8 eV. However, we cannot rule out the possibility that the Ga<sup>I</sup> curve is somewhat deeper than that of

Ga<sup>III</sup>, in which case the edge shift would be considerably less.

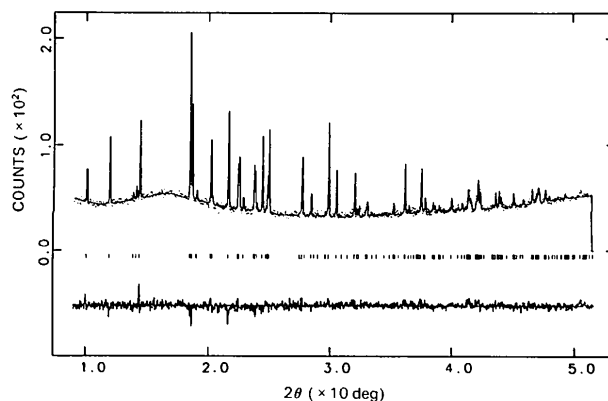
Preliminary photoelectron spectroscopy results (Shen & Wilkinson, 1989) show that the relative shift in edge position for states with a binding energy of less than 1240 eV is only about 1.8 eV, and that Ga<sup>I</sup> is indeed more readily ionizable than Ga<sup>III</sup>. By comparison, the difference between Ga metal and Ga<sub>2</sub>O<sub>3</sub>



(a)



(b)



(c)

Fig. 1. Observed (dots), calculated (smooth curve) and difference profiles for GaCl<sub>2</sub> at wavelengths of (a) 1.2478, (b) 1.1964 and (c) 1.1957 Å. Reflection markers are also shown.

Table 4. Refined values of  $f'$  for  $\text{GaCl}_2$  at different energies

$E$ (eV)	$f'$ (constrained)	$f'$ ( $\text{Ga}^{\text{I}}$ )	$f'$ ( $\text{Ga}^{\text{III}}$ )
9933.9	-3.8 (3)		
9936.1		-3.4 (1)	-3.3 (1)
9937.3*		-3.9 (2)	-3.8 (2)
10143.8	-3.8 (2)		
10312.4	-4.1 (3)		
10352.8	-5.8 (2)		
10353.2		-7.5 (1)	-7.1 (1)
10354.6		-7.2 (1)	-7.2 (1)
10359.8	-8.9 (2)		
10363.3	-8.3 (1)		
10365.5		-10.5 (1)	-8.8 (1)
10369.5		-10.6 (2)	-8.7 (3)
		-12.9 (1)	-9.7 (2)

\* The lattice constants from this data set were used for wavelength calibration for all the reported refinements.

is about 1.9 eV (Schön, 1973). However, photoelectron spectroscopic data are not a reliable guide to the magnitude of an oxidation-state shift at the X-ray absorption edge because the near-edge features in an X-ray absorption spectrum correspond to transitions to bound states rather than the production of a photoelectron. An estimated absorption-edge shift of 8 eV is by no means inconsistent with the photoelectron spectroscopy data; indeed, it has previously

been noted that X-ray absorption-edge shifts are often much larger than those observed in photoelectron spectra (Manthiram, Sarode, Madhusudan, Gopalakrishnan & Rao, 1980).

For a more detailed interpretation of oxidation-state contrast measurements, reliable data on the expected behaviour of  $f'(E)$  and  $f''(E)$  are required. The lack of such data is a potential problem for many anomalous-scattering experiments. A number of methods can be used to determine  $f'(E)$  and  $f''(E)$  curves. Theoretical calculations have recently been reviewed by Creagh (1988). The widely used values of Cromer & Liberman for free atoms, based upon a relativistic dipole theory (Cromer & Liberman, 1970, 1981), are in good agreement with experiment except in the vicinity of an absorption edge, since these calculations do not take into account fine structure such as near-edge effects and EXAFS. Strong near-edge effects commonly occur at  $L_{\text{II}}$  and  $L_{\text{III}}$  edges, and have been observed for some  $K$  and  $L_1$  edges.

Several experimental methods for the determination of  $f'(E)$  and  $f''(E)$  are also available. These include X-ray interferometry (Hart & Siddons, 1981; Bonse & Hartmann-Lotsch, 1984; Begum, Hart, Lea & Siddons, 1986), the application of the Kramers-Kronig relation to absorption data (Bonse & Hartmann-Lotsch, 1984; Hoyt, De Fontaine & Warburton, 1984; Dreier, Rabe, Malzfeldt & Neimann, 1984), absolute powder intensity methods (Suortti, Hastings & Cox, 1985) and crystallographic refinement using a known structure, either with single crystals (Templeton & Templeton, 1978, 1982, 1985, 1988, 1990; Phillips, Templeton, Templeton & Hodgson, 1978; Templeton, Templeton & Phizackerley, 1980; Templeton, Templeton, Phillips & Hodgson, 1980; Templeton, Templeton, Phizackerley & Hodgson, 1982), or with powders (Will, Masciocchi, Hart & Parrish, 1987). The crystallographic methods are the only ones that offer the possibility of site-specific determinations for complex materials.

When using experimental data obtained by any of the above techniques, it is necessary to consider what effect different instrumental arrangements have on the observed form of  $f'(E)$  and  $f''(E)$ , and also how these functions might be expected to vary between different compounds. The energy resolution used in an experiment influences the shape of the observed  $f'(E)$  and  $f''(E)$  curves because the instrument bandpass is convoluted with the natural shape. This should be taken into account when data from different sources are being used together (Lee, Gao, Sheu, Petricek, Restori, Coppens, Darovskikh, Phillips, Sleight & Subramanian, 1989). The influence of instrument bandpass is well illustrated by two studies carried out on the compound  $\text{NaSmC}_{10}\text{H}_{12}\text{N}_2\text{O}_8 \cdot 8\text{H}_2\text{O}$  at the  $L_{\text{III}}$  edge of Sm

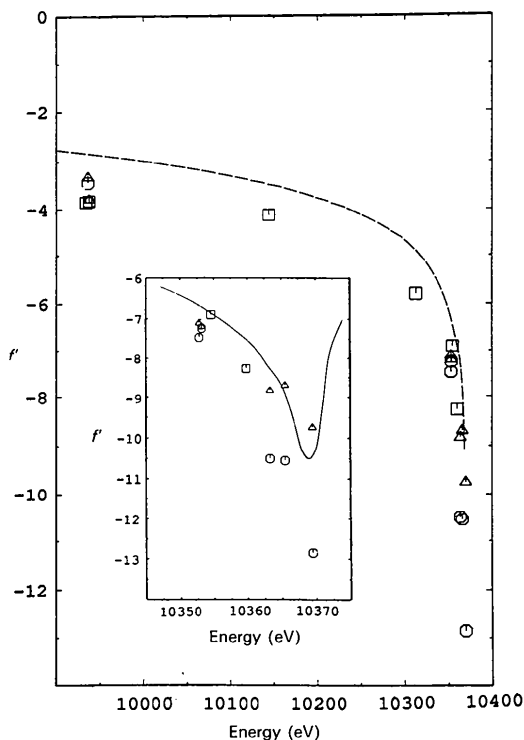


Fig. 2. The variation of  $f'$  with energy, showing Cromer & Liberman values (dotted line) shifted to match the edge position, average values from  $\text{GaCl}_2$  (squares),  $f'(\text{Ga}^{\text{I}})$  (circles), and  $f'(\text{Ga}^{\text{III}})$  (triangles). The inset compares the present findings with the values for GaAs reported by Fukamachi *et al.* (1977) (solid line); the latter curve was again shifted to match the edge position.

(Templeton, Templeton & Phizackerley, 1980; Templeton, Templeton, Phizackerley & Hodgson, 1982). A difference of up to 8 e is seen in both  $f'$  and  $f''$  for the two experiments. The transferability of  $f'(E)$  and  $f''(E)$  between compounds is also dependent upon the similarity of the absorption cross-sections for the different materials.

Near-edge structure, such as the white-line features commonly found at  $L_{II}$  and  $L_{III}$  edges (Brown, Peierls & Stern, 1977), depend upon final-state density-of-state effects or the presence of Rydberg-type core excitonic states, and may be expected to vary from compound to compound. It has been suggested that this chemical dependence of near-edge structure effectively prevents the quantitative transfer of scattering-factor information in the case of  $L_{II}$  and  $L_{III}$  edges (Lye, Phillips, Kaplan, Doniach & Hodgson, 1980). Furthermore, Templeton & Templeton (1988) reported a value of  $-11.6$  e for  $f'$  at the  $K$  edge of  $Zn^{2+}$  in zinc tartrate, compared to less than  $-9$  e for Zn metal, showing that chemical environment can be responsible for more than just an edge shift. In addition to this, the presence of EXAFS implies that anomalous-scattering factors are dependent upon the local structure around an absorbing species. This has been observed in many determinations of  $f'(E)$  and  $f''(E)$ . The presence of EXAFS-related structure in  $f'(E)$  and  $f''(E)$  is unlikely to prevent the transfer of data between compounds as it is a relatively small effect, particularly for heavier elements (Dreier, Rabe, Malzfeldt & Neimann, 1984) and mainly influences the region above the absorption edge. Owing to these problems, values of  $f'(E)$  and  $f''(E)$  obtained from the compound under study, or from closely related model materials, should be used where possible. It is important that data should be obtained using the same instrumental bandpass, or that account be taken of the latter.

Given the above limitations on the use of experimental information, our estimated shift of 8 eV should be treated with caution. The absorption spectrum of GaAs shows the presence of near-edge structure on the Ga  $K$  edge (Fukamachi & Hosoya, 1975; Fukamachi, Hosoya, Kawamura & Okunuki, 1977), which may be significantly different for  $Ga^I$  and  $Ga^{III}$  in  $GaCl_2$  and could have a large influence on the observed result. Further experiments to measure the X-ray absorption spectra of  $GaCl_2$  and model compounds such as  $GaAlCl_4$ ,  $KGaCl_4$  and  $GaCl_3$  are planned in order that such effects can be examined.

### Concluding remarks

We have demonstrated that it is possible, with powder diffraction techniques, to observe a difference in the  $f'(E)$  curves for two different ox-

idation states of an element in a mixed-valence compound, in the vicinity of an appropriate absorption edge. The interpretation of this difference in terms of a relative absorption-edge shift is difficult, but should be possible if suitable reference data are available. This method potentially provides information similar to that available from XANES studies, but with the advantage of being site selective. Ideally, reference data should be collected under identical conditions on model compounds, but in practice this approach is likely to be too time consuming. Alternatively, the Kramers–Kronig transformation of X-ray absorption data offers a convenient route to such information.

We thank A. M. Chippindale and N. J. Stedman for help with the data collection. This work was supported by Shell (Amsterdam) and the Division of Materials Sciences, US Department of Energy, under contract DE-AC02-76CH00016. APW is grateful to the SERC for the provision of a studentship.

### References

- ABRAHAMS, S. C. & KEVE, E. T. (1971). *Acta Cryst.* **A27**, 157–165.  
 ATTFIELD, J. P. (1990). *Nature (London)*, **343**, 46–49.  
 BEGUM, R., HART, M., LEA, K. R. & SIDONS, D. P. (1986). *Acta Cryst.* **A42**, 456–464.  
 BONSE, U. & HARTMANN-LOTSCH, I. (1984). *Nucl. Instrum. Methods*, **222**, 185–188.  
 BROWN, M., PEIERLS, R. E. & STERN, E. A. (1977). *Phys. Rev. B*, **15**, 738–744.  
 CREAGH, D. C. (1988). *Aust. J. Phys.* **41**, 487–501.  
 CROMER, D. T. & LIBERMAN, D. (1970). *J. Chem. Phys.* **53**, 1891–1898.  
 CROMER, D. T. & LIBERMAN, D. (1981). *Acta Cryst.* **A37**, 267–268.  
 DREIER, P., RABE, P., MALZFELDT, W. & NEIMANN, W. (1984). *J. Phys. C*, **17**, 3123–3136.  
 FUKAMACHI, T. & HOSOYA, S. (1975). *Acta Cryst.* **A31**, 215–220.  
 FUKAMACHI, T., HOSOYA, S., KAWAMURA, T. & OKUNUKI, M. (1977). *Acta Cryst.* **A33**, 54–58.  
 GARTON, G. & POWELL, H. M. (1957). *J. Inorg. Nucl. Chem.* **4**, 84–89.  
 HART, M. & SIDONS, D. P. (1981). *Proc. R. Soc. London Ser. A*, **376**, 465–482.  
 HOWLAND, R. S., GEBALLE, T. H., LADERMAN, S. S., FISCHER-COLBRIE, A., SCOTT, M., TARASCON, J. M. & BARBOUX, P. (1989). *Phys. Rev. B*, **39**, 9017–9027.  
 HOYT, J. J., DE FONTAINE, D. & WARBURTON, W. K. (1984). *J. Appl. Cryst.* **17**, 344–351.  
 KWEI, G. H., VON DREELE, R. B., WILLIAMS, A., GOLDSTONE, J. A., LAWSON, A. C. II & WARBURTON, W. K. (1990). *J. Mol. Struct.* **223**, 384–406.  
 LARSON, A. C. & VON DREELE, R. B. (1987). Report No. LA-UR-86-748. Los Alamos Laboratory, Los Alamos, USA.  
 LEE, P., GAO, Y., SHEU, H. S., PETRICEK, V., RESTORI, R., COPPENS, P., DAROVSKIKH, A., PHILLIPS, J. C., SLEIGHT, A. W. & SUBRAMANIAN, M. A. (1989). *Science*, **244**, 62–63.  
 LYE, R. C., PHILLIPS, J. C., KAPLAN, D., DONIACH, S. & HODGSON, K. O. (1980). *Proc. Natl Acad. Sci. USA*, **77**, 5884–5888.  
 MANTHIRAM, A., SARODE, P. R., MADHUSUDAN, W. H., GOPALAKRISHNAN, J. & RAO, C. N. R. (1980). *J. Phys. Chem.* **84**, 2200–2203.

- MORONEY, L. M., THOMPSON, P. & COX, D. E. (1988). *J. Appl. Cryst.* **21**, 206–208.
- PHILLIPS, J. C., TEMPLETON, D. H., TEMPLETON, L. H. & HODGSON, K. O. (1978). *Science*, **210**, 257–259.
- SCHMIDBAUR, H., NOWAK, R., BUBLAK, W., BURKET, P., HUBER B. & MÜLLER, G. (1987). *Z. Naturforsch. Teil B*, **42**, 553–556.
- SCHÖN, G. (1973). *J. Electron Spectrosc. Relat. Phenom.*, **2**, 75–86.
- SHEN, B. & WILKINSON, A. P. (1989). Unpublished results.
- SUORTTI, P., HASTINGS, J. B. & COX, D. E. (1985). *Acta Cryst.* **A41**, 417–420.
- TEMPLETON, D. H. & TEMPLETON, L. K. (1982). *Acta Cryst.* **A38**, 62–67.
- TEMPLETON, D. H. & TEMPLETON, L. K. (1985). *Acta Cryst.* **A41**, 133–142.
- TEMPLETON, D. H., TEMPLETON, L. K., PHILLIPS, J. C. & HODGSON, K. O. (1980). *Acta Cryst.* **A36**, 436–442.
- TEMPLETON, L. K. & TEMPLETON, D. H. (1978). *Acta Cryst.* **A34**, 368–371.
- TEMPLETON, L. K. & TEMPLETON, D. H. (1988). *J. Appl. Cryst.* **21**, 558–561.
- TEMPLETON, L. K. & TEMPLETON, D. H. (1990). *J. Appl. Cryst.* **23**, 18–20.
- TEMPLETON, L. K., TEMPLETON, D. H. & PHIZACKERLEY, R. P. (1980). *J. Am. Chem. Soc.* **102**, 1185–1186.
- TEMPLETON, L. K., TEMPLETON, D. H., PHIZACKERLEY, R. P. & HODGSON, K. O. (1982). *Acta Cryst.* **A38**, 74–78.
- WILL, G., MASCIOCCHI, N., HART, M. & PARRISH, W. (1987). *Acta Cryst.* **A43**, 677–683.
- WILLIAMS, A., KWEL, G. H., ORTIZ, A. T., KARNOWSKI, M. & WARBURTON, W. K. (1990). *J. Mater. Res.* In the press.

*Acta Cryst.* (1991). **B47**, 161–166

## High-Resolution Neutron Powder Diffraction Studies\* of the Structure of CsDSO<sub>4</sub>

BY A. V. BELUSHKIN

*Joint Institute for Nuclear Research, 141980 Dubna, USSR*

W. I. F. DAVID AND R. M. IBERSON

*Rutherford Appleton Laboratory, Chilton, Didcot, Oxon OX11 0QX, England*

AND L. A. SHUVALOV

*Institute of Crystallography, 117333 Moscow, USSR*

(Received 1 April 1990; accepted 24 September 1990)

### Abstract

High-resolution neutron powder diffraction data were used to determine the crystal structure of the superionic conductor CsDSO<sub>4</sub> at 300 K (low-conductivity phase) and at 448 K (superionic phase). A full structural analysis was performed, using the Rietveld method, to obtain previously unknown atomic positions, site occupancies and temperature factors for the light atoms. The mechanism of deuterium diffusion is discussed. At 300 K: monoclinic,  $P2_1/c$ ,  $a = 7.78013$  (9),  $b = 8.13916$  (2),  $c = 7.72187$  (9) Å,  $\beta = 110.8720$  (4)°,  $R_{wp} = 4.19\%$  for 7331 profile points (844 reflections). At 448 K: tetragonal,  $I4_1/amd$ ,  $a = 5.74147$  (9),  $c = 14.31508$  (26) Å,  $R_{wp} = 2.21\%$  for 8289 profile points (194 reflections).

### 1. Introduction

Deuterated caesium hydrogen sulfate, CsDSO<sub>4</sub>, belongs to a class of crystalline compounds which

have hydrogen bonds of the type  $MXAO_4$  ( $M = \text{Cs, Rb}$ ;  $X = \text{H, D}$ ;  $A = \text{S, Se}$ ). All these materials undergo a phase transition to a superionic state. The phase transition is characterized by a sharp increase in conductivity (by three to four orders of magnitude, up to  $10^{-2} \Omega^{-1} \text{cm}^{-1}$ ) and by a large spontaneous shear strain ( $10^{-2}$ ) (Baranov, Shuvalov & Schagina, 1982, 1984; Baranov, Shuvalov, Fedosyuk & Schagina, 1984; Yokota, 1982). The transition temperature ( $T_c$ ) for CsDSO<sub>4</sub> is 412 K (Baranov, Shuvalov & Schagina, 1984). Previous X-ray and neutron diffraction data showed the phase (II) structure, below  $T_c$ , to be monoclinic, space group  $P2_1/c$ , and the phase (I) structure, above  $T_c$ , to be tetragonal, space group  $I4_1/amd$  (Merinov, Baranov, Maksimov & Shuvalov, 1986; Balagurov, Beskrovnyi & Savenko, 1987; Merinov, Baranov, Shuvalov & Maksimov, 1987). The crystal structures of CsDSO<sub>4</sub> (I) and CsDSO<sub>4</sub> (II) are isomorphic with the corresponding phases of CsHSO<sub>4</sub>, CsHSeO<sub>4</sub> and CsDSeO<sub>4</sub> (Balagurov, Belushkin & Beskrovnyi, 1985; Belushkin, Natkaniec, Plakida, Shuvalov & Wasicki, 1987). It is therefore believed that conclusions as to the crystal structure and mechanism of conductivity

\* The investigation was performed at the Rutherford Appleton Laboratory, England, and at the Laboratory of Neutron Physics, Dubna, USSR.